nature medicine

Blockade of receptor activator of nuclear factor-κB (RANKL) signaling improves hepatic insulin resistance and prevents development of diabetes mellitus

Stefan Kiechl[1,16], Jürgen Wittmann[2], Andrea Giaccari[3,4], Michael Knoflach[1], Peter Willeit[1,5], Aline Bozec[6], Alexander R Moschen[7], Giovanna Muscogiuri[3], Gian Pio Sorice[3], Trayana Kireva[6], Monika Summerer[8], Stefan Wirtz[9], Julia Luther[6], Dirk Mielenz[2], Ulrike Billmeier[9], Georg Egger[10], Agnes Mayr[11], Friedrich Oberhollenzer[10], Florian Kronenberg[8], Michael Orthofer[12], Josef M Penninger[12], James B Meigs[13,14], Enzo Bonora[15], Herbert Tilg[7], Johann Willeit[1] & Georg Schett[6,16]

Hepatic insulin resistance is a driving force in the pathogenesis of type 2 diabetes mellitus (T2DM) and is tightly coupled with excessive storage of fat and the ensuing inflammation within the liver[1–3]. There is compelling evidence that activation of the transcription factor nuclear factor-κB (NF-κB) and downstream inflammatory signaling pathways systemically and in the liver are key events in the etiology of hepatic insulin resistance and β-cell dysfunction, although the molecular mechanisms involved are incompletely understood[3–6]. We here test the hypothesis that receptor activator of NF-κB ligand (RANKL), a prototypic activator of NF-κB, contributes to this process using both an epidemiological and experimental approach. In the prospective population-based Bruneck Study, a high serum concentration of soluble RANKL emerged as a significant ($P < 0.001$) and independent risk predictor of T2DM manifestation. In close agreement, systemic or hepatic blockage of RANKL signaling in genetic and nutritional mouse models of T2DM resulted in a marked improvement of hepatic insulin sensitivity and amelioration or even normalization of plasma glucose concentrations and glucose tolerance. Overall, this study provides evidence for a role of RANKL signaling in the pathogenesis of T2DM. If so, translation to the clinic may be feasible given current pharmacological strategies to lower RANKL activity to treat osteoporosis.

RANKL (also known as TNFSF11) is a member of the tumor necrosis factor superfamily and, after ligation with its cognate receptor RANK (also known as TNFRSF11a), is a potent stimulator of NF-κB. Notably, both RANKL and RANK are expressed in human liver tissue and pancreatic β-cells[7], and concentrations of the soluble decoy receptor osteoprotegerin (OPG), considered to be a reliable surrogate for the overall activity of this cytokine network, are elevated in patients with T2DM, especially in those with poor glycemic control and complicated disease course[8–11]. RANKL exists in both membrane-bound and biologically active soluble forms, with the latter originating from secretion and cleavage[9,12]. Concentrations of soluble RANKL are elevated in or predictive of various human diseases, including cardiovascular disease, nontraumatic fractures, multiple myeloma, rheumatoid arthritis and inflammatory bowel disease[8–11,13–18]. We determined the distribution of serum concentrations of RANKL and OPG in our study population ($n = 844$) (**Supplementary Fig. 1a**). Soluble RANKL concentrations showed associations with insulin resistance assessed by homeostasis model (HOMA-IR) and Gutt Index values and with the number of metabolic syndrome components clustering in an individual (**Supplementary Data**) but were not related to most standard population characteristics (**Supplementary Table 1**).

Between 1990 and 2005, 78 of the 844 individuals in the study population (9.2%) developed T2DM (incidence rate, 7.2 per 1,000 person years (95% confidence interval (CI) 5.7–8.9)). We determined the baseline characteristics of subjects with and without incident T2DM (**Supplementary Table 2**) and found that the concentrations of soluble RANKL differed considerably between the two groups. In a pooled logistic regression analysis adjusted for age, sex and period

[1]Department of Neurology, Medical University Innsbruck, Innsbruck, Austria. [2]Department of Internal Medicine 3, Division of Molecular Immunology, University of Erlangen-Nuremberg, Erlangen, Germany. [3]Division of Endocrinology and Metabolic Diseases, Università Cattolica del Sacro Cuore, Policlinico 'A. Gemelli', Rome, Italy. [4]Fondazione Don Gnocchi, Milan, Italy. [5]Department of Public Health and Primary Care, University of Cambridge, Cambridge, UK. [6]Department of Internal Medicine 3, University of Erlangen-Nuremberg, Erlangen, Germany. [7]Department of Medicine I, Division of Endocrinology, Gastroenterology and Metabolism, Medical University Innsbruck, Innsbruck, Austria. [8]Department of Medical Genetics, Division of Genetic Epidemiology, Molecular and Clinical Pharmacology, Medical University Innsbruck, Innsbruck Austria. [9]Department of Internal Medicine I, University of Erlangen-Nuremberg, Erlangen, Germany. [10]Department of Internal Medicine, Bruneck Hospital, Bruneck, Italy. [11]Department of Laboratory Medicine, Bruneck Hospital, Bruneck, Italy. [12]Institute of Molecular Biotechnology of the Austrian Academy of Sciences (IMBA), Vienna, Austria. [13]Department of Internal Medicine, Harvard University, Boston, Massachusetts, USA. [14]Department of Medicine, General Medicine Division, Massachusetts General Hospital, Boston, Massachusetts, USA. [15]Division of Endocrinology, Diabetes and Metabolic Diseases, University and Hospital Trust of Verona, Verona, Italy. [16]These authors contributed equally to this work. Correspondence should be addressed to S.K. (stefan.kiechl@i-med.ac.at) or G.S. (georg.schett@uk-erlangen.de).

Received 25 October 2012; accepted 8 January 2013; published online 10 February 2013; doi:10.1038/nm.3084

Table 1 Risk of incident T2DM according to concentration of soluble RANKL in the prospective Bruneck Study.

	Tertile group for RANKL					
	Low	Medium	High			
Median	0.60	1.00	1.60			
Range	0.10–0.80	0.85–1.25	1.30–16.95			
Number of events (incident T2DM)	19	29	30			
Person years of follow up	3,664.4	3,476.3	3,752.3			
Incidence rate per 1,000 person years (95% CI) based on baseline RANKL concentration	5.2 (3.1–8.1)	8.3 (5.6–12.0)	8.0 (5.4–11.4)			
Incidence rate per 1,000 person years (95% CI) based on updated RANKL concentration[a]	2.7 (1.3–5.0)	8.0 (5.4–11.5)	10.9 (7.8–14.9)			
	OR (95% CI) of incident T2DM			P_{trend}	OR (95% CI) for a 1 s.d. higher concentration of RANKL	*P*
Pooled logistic regression, 1990–2005 (*n* = 2,278)[b]						
Adjusted for age, sex and period	1.00	3.37 (1.63–6.97)	4.06 (2.01–8.20)	<0.001	1.96 (1.54–2.49)	<0.001
Multivariate adjustment (model 1)[c]	1.00	3.41 (1.64–7.07)	4.19 (2.07–8.48)	<0.001	1.94 (1.52–2.46)	<0.001
Multivariate adjustment (model 2)[c]	1.00	3.13 (1.50–6.53)	4.04 (1.98–8.22)	<0.001	1.86 (1.45–2.38)	<0.001
Multivariate adjustment (model 3)[c]	1.00	3.01 (1.40–6.47)	4.23 (2.03–8.81)	0.001	1.91 (1.47–2.49)	<0.001
Multivariate adjustment (model 4)[c]	1.00	3.05 (1.41–6.59)	4.26 (2.04–8.92)	0.001	1.94 (1.48–2.54)	<0.001
HbA1c-based definition of T2DM[d]	1.00	3.28 (1.58–6.82)	4.02 (1.97–8.20)	<0.001	1.82 (1.41–2.34)	<0.001
Extended follow up, 1990–2010 (*n* = 2,852)[e]						
Adjusted for age, sex and period	1.00	3.78 (1.90–7.52)	5.17 (2.69–9.94)	<0.001	1.91 (1.55–2.36)	<0.001
Multivariate adjustment (model 1)[c]	1.00	3.84 (1.93–7.63)	5.29 (2.75–10.2)	<0.001	1.90 (1.54–2.35)	<0.001
Multivariate adjustment (model 2)[c]	1.00	3.55 (1.77–7.08)	5.15 (2.66–9.97)	<0.001	1.85 (1.49–2.29)	<0.001
Multivariate adjustment (model 3)[c]	1.00	3.49 (1.70–7.14)	5.97 (3.01–11.8)	<0.001	1.93 (1.54–2.43)	<0.001

[a]In this analysis, subjects were attributed to RANKL tertile groups according to RANKL concentrations measured in 1990, 1995 and 2000 (that is, individuals were allowed to change RANKL tertile groups during follow up). The numbers of events in the three groups were 10, 29 and 39; the person years of follow up were 3,704.5, 3,613.9 and 3,574.7. [b]ORs (95% CI) were derived from pooled logistic regression analyses and calculated for a 1 s.d. unit higher $\log_e$-transformed soluble RANKL concentration (right columns) and in separate models for RANKL tertile groups (left columns). The bottom tertile group served as the reference category. Base models were adjusted for age, sex and period of follow up (1990–1995, 1995–2000 or 2000–2005). ORs reflect the risk of new-onset T2DM in a 5-year period. All covariates were updated every 5 years. [c]The analysis was further adjusted for social status, cigarette smoking, alcohol consumption, physical activity and family history for diabetes (model 1), plus body mass index and waist-to-hip ratio (model 2), plus fasting glucose and $\log_e$-transformed concentration of hsCRP (model 3), plus common types of medication (statins, β-blockers, diuretics, calcium channel blockers, angiotensin-converting enzyme and angiotensin receptor inhibitors, corticosteroids, digitalis drugs, platelet inhibitors, oral anticoagulation and hormone replacement therapy, each considered a separate variable) (model 4). [d]Diabetes was defined by a physician- and record-confirmed disease status or HbA1c ≥6.5%. Analysis was performed by pooled logistic regression and based on 2,273 observation periods and 78 cases of incident T2DM (model 2). As with the main analysis, subjects with diabetes at baseline (according to these alternate criteria) were excluded. [e]These analyses focused on the extended follow up between 1990 and 2010 (*n* = 2,852 observation periods) and considered 100 cases of incident T2DM. Because RANKL concentration was not measured from the blood samples collected in 2005, RANKL concentrations assessed from the samples collected in 2000 were used to predict T2DM risk both in the 2000–2005 and 2005–2010 periods of follow up.

of follow up, soluble RANKL concentration was significantly associated with T2DM risk such that higher concentrations conferred elevated risk (odds ratio (OR) = 3.37 (95% CI 1.63–6.97) and OR = 4.06 (95% CI 2.01–8.20) for a comparison between the middle and top, respectively, compared to the bottom tertile group; $P < 0.001$) (**Table 1**). In multivariable analyses, we progressively adjusted for lifestyle factors (model 1) and measures of body composition (model 2). The results did not change appreciably when using these two models (**Table 1**). When interpreting this finding, it must be considered that body weight and composition, although being well-established risk factors for glucose abnormalities, explained only a minor proportion of T2DM risk (~5%) in our population aged 40–100 years, as a comparatively low (7.5%) proportion of these individuals were obese. Details on the predictive accuracy of soluble RANKL are summarized in the **Supplementary Data**.

We performed a number of ancillary analyses to further substantiate our findings. Additional adjustments for fasting glucose (glycated hemoglobin (HbA1c)) and $\log_e$-transformed high-sensitivity C-reactive protein (hsCRP) (model 3) and for hormone replacement therapy and standard cardiovascular drugs (model 4), some of which had been shown to be related with RANKL activity[9,19], had little effect on the results (**Table 1**). The association between RANKL and T2DM was internally consistent in the three periods of follow up and in the subgroups (**Supplementary Table 3**). When using alternative diagnostic criteria for T2DM or extending the follow up to 20 years (1990–2010; incident T2DM, $n = 100$), the findings were similar (**Table 1**). Unlike with most other markers of inflammation, the association between RANKL and T2DM was not attenuated by multivariable adjustment and maintained significance even after accounting for the multiple comparisons performed (**Supplementary Table 4**). In contrast to RANKL, the serum concentration of OPG was unrelated to T2DM risk (**Supplementary Table 5**). However, we found an increase in OPG concentration with or after occurrence of T2DM, which was associated with a modest decline in free soluble RANKL concentration (**Supplementary Fig. 1b**).

In search of the mechanistic link between RANKL and T2DM, we hypothesized that the liver is the key target organ of RANKL signaling in this context. We engineered hepatocyte-specific *Rank* knockout ($Rank^{LKO}$) mice and compared them with floxed-allele littermate controls ($Rank^{WT}$ mice) (**Fig. 1**). Whereas $Rank^{WT}$ mice developed insulin resistance after 4 weeks of a high-fat diet (HFD), $Rank^{LKO}$ mice did not, and $Rank^{LKO}$ mice showed fasting glucose and insulin concentrations that were similar to those of $Rank^{WT}$ mice fed a normal-fat diet (NFD) (**Fig. 1a**). We obtained similar results when liver expression of Rank was downregulated by hydrodynamic injection of *Rank* shRNA (RANKi) lentiviral vectors (**Fig. 1b;** for vector details see **Supplementary Fig. 2**)[20–23]. Of note, RANKi vector administration achieved tissue-specific blockade of Rank expression

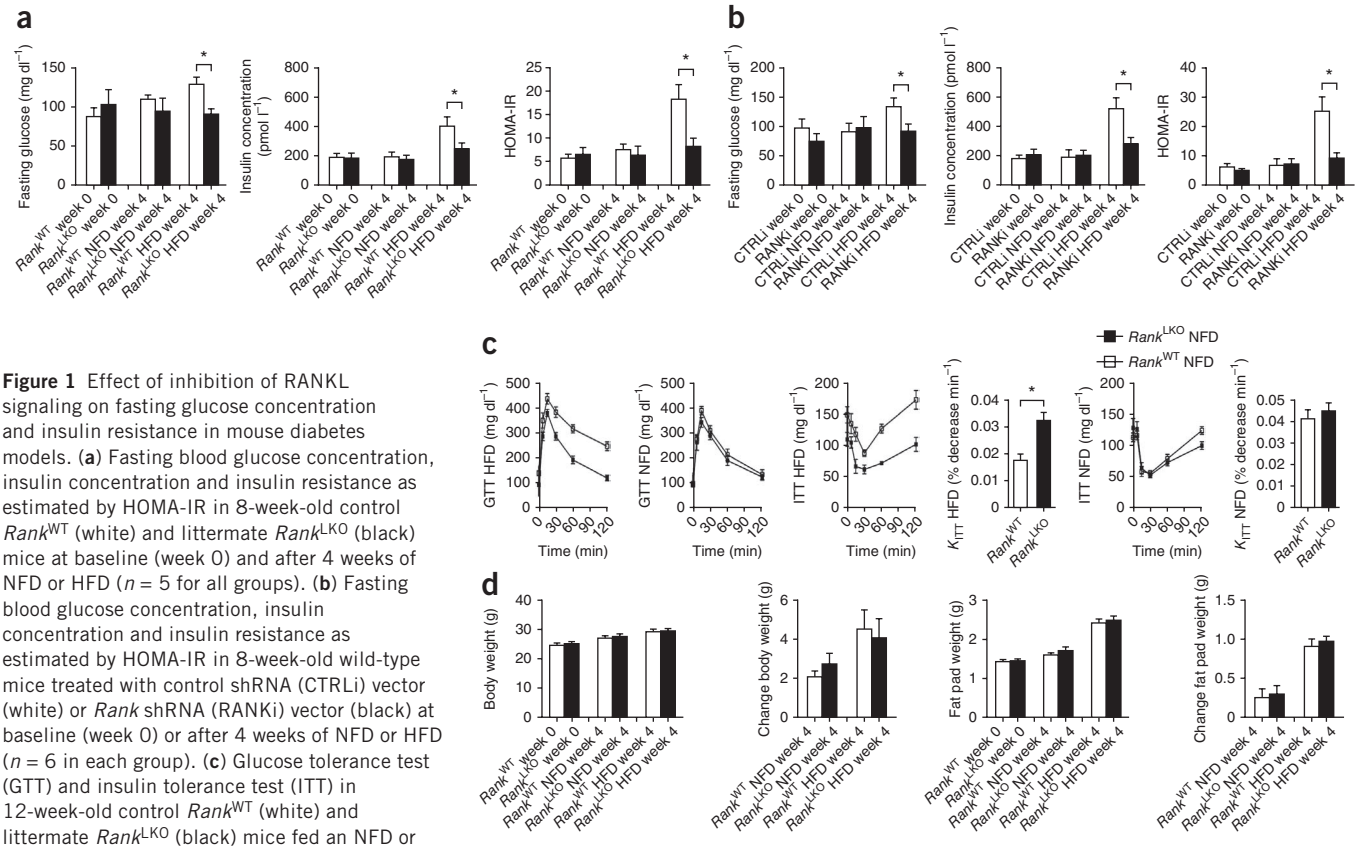

Figure 1 Effect of inhibition of RANKL signaling on fasting glucose concentration and insulin resistance in mouse diabetes models. (**a**) Fasting blood glucose concentration, insulin concentration and insulin resistance as estimated by HOMA-IR in 8-week-old control *Rank*^{WT} (white) and littermate *Rank*^{LKO} (black) mice at baseline (week 0) and after 4 weeks of NFD or HFD ($n = 5$ for all groups). (**b**) Fasting blood glucose concentration, insulin concentration and insulin resistance as estimated by HOMA-IR in 8-week-old wild-type mice treated with control shRNA (CTRLi) vector (white) or *Rank* shRNA (RANKi) vector (black) at baseline (week 0) or after 4 weeks of NFD or HFD ($n = 6$ in each group). (**c**) Glucose tolerance test (GTT) and insulin tolerance test (ITT) in 12-week-old control *Rank*^{WT} (white) and littermate *Rank*^{LKO} (black) mice fed an NFD or HFD ($n = 5$ for all groups). K_{ITT}, calculated plasma glucose disappearance rate. (**d**) Body weight (left) and epididymal fat pad weight (right) in 8-week-old control *Rank*^{WT} (white) and *Rank*^{LKO} (black) mice at baseline (week 0) and after 4 weeks of NFD or HFD ($n = 5$ for all groups). Data are shown as the means ± s.e.m. *$P < 0.05$ compared to controls calculated using the Mann Whitney *U* test.

comparable to that resulting from hepatocyte-specific genetic deletion of *Rank* (**Supplementary Fig. 3**). We also performed glucose tolerance tests on the two groups of mice (**Fig. 1c**). Insulin tolerance tests showed significantly higher insulin sensitivity in *Rank*^{LKO} compared to *Rank*^{WT} mice fed an HFD ($P = 0.019$; **Fig. 1c**). Body and epididymal fat pad weight, as well as weight gain under HFD, were similar in *Rank*^{WT} and *Rank*^{LKO} mice (**Fig. 1d**). Mice with a specific deletion of *Rank* in the skeletal muscle (Msk-Cre; *Rank*^{flox}) or in pancreatic β-cells (RIP-Cre; *Rank*^{flox}) did not show improved insulin sensitivity compared to littermate controls when fed an HFD (data not shown).

In addition, we crossbred leptin-deficient (*ob/ob*) mice, another animal model of insulin resistance and hyperglycemia, with *Rank*^{LKO} mice, and the resulting *Rank*^{LKO} *ob/ob* mice had significantly lower fasting glucose concentrations ($P = 0.027$) and HOMA-IR values ($P = 0.023$) than *Rank*^{WT} *ob/ob* mice (**Supplementary Fig. 4a**). We achieved similar effects by hydrodynamic injection of RANKi vectors in *ob/ob* mice, which reduced fasting glucose and insulin concentrations and ameliorated insulin resistance ($P = 0.004$) (**Supplementary Fig. 4b**). In line with this, blockade of RANKL signaling by systemic application of its decoy receptor Opg improved glucose metabolism in *ob/ob* mice (**Supplementary Fig. 4c**).

We used euglycemic-hyperinsulinemic clamp studies to further scrutinize the effects of RANKL signaling on hepatic insulin resistance. In *Rank*^{LKO} and *Rank*^{WT} mice fed an NFD, insulin infusion effectively decreased hepatic glucose production (**Fig. 2a**). This insulin effect was significantly impaired in *Rank*^{WT} mice fed an HFD but was restored in *Rank*^{LKO} mice on an HFD ($P = 0.012$; **Fig. 2a**). We obtained similar findings when blocking *Rank* by RANKi vectors (**Fig. 2b**), which extended to insulin signaling in liver tissue showing normal phosphorylation of Akt in *Rank*^{LKO} but not *Rank*^{WT} mice fed an HFD (**Fig. 2c**). Moreover, *Rank*^{LKO} mice had lower excess triglyceride and cholesterol content than liver tissue from *Rank*^{WT} mice fed an HFD (**Supplementary Fig. 5a**), and *Rank* blockade by RANKi vectors inhibited NF-κB activation. Accordingly, phosphorylation of IκB kinases (IKKs), as well as of downstream RelA (also known as p65), was abrogated by downregulation of Rank expression (**Fig. 2d**).

We then performed *in vitro* studies of cultured mouse hepatocytes challenged with mouse RANKL. Hepatocytes stably expressed mRNA encoding Rank, and stimulation of hepatocytes with RANKL resulted in a prominent upregulation of NF-κB–inducible tumor necrosis factor α (TNF-α), interleukin-1 (IL-1) and chemokine (C-X-C motif) ligand 1 (CXCL1) (**Supplementary Fig. 5b**). RANKL-mediated upregulation of proinflammatory genes was completely dependent on NF-κB activation and was blocked by pretreatment of hepatocytes with the IKK-β–specific inhibitor AS602868 (**Supplementary Fig. 5c**). We also tested whether RANKL stimulation of hepatocytes could induce activation of Kupffer cells[24]. RANKL induced TNF-α expression and release in hepatocytes isolated from *Rank*^{WT} but not *Rank*^{LKO} mice (**Fig. 3a**). When incubating Kupffer cells with the supernatants of RANKL-stimulated hepatocytes from *Rank*^{WT} mice, expression of mRNA encoding TNF-α, IL-1, IL-6 and IL-10 in Kupffer cells was amplified (**Fig. 3b**). In contrast, supernatant from unstimulated hepatocytes and RANKL-stimulated hepatocytes from *Rank*^{LKO} mice did not induce cytokine expression by Kupffer cells.

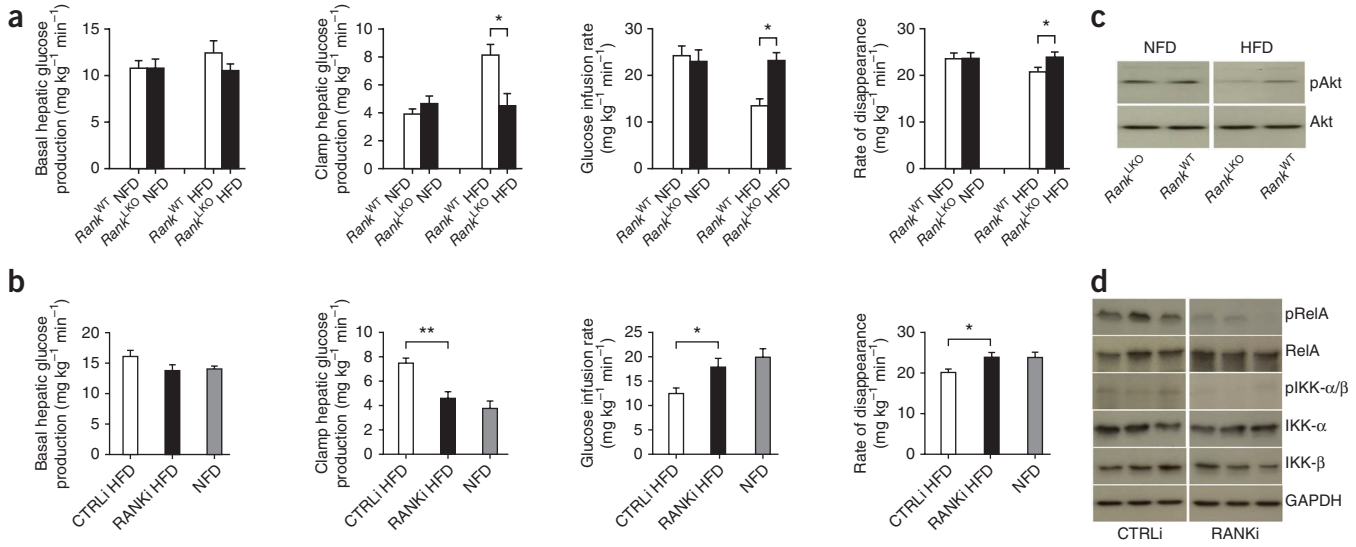

Figure 2 Effects of inhibition of Rank on hepatic glucose production, insulin signaling and NF-κB activation. (**a**) Euglycemic-hyperinsulinemic clamp procedure in 12-week-old control *Rank*^{WT} (white) and littermate *Rank*^{LKO} (black) mice fed an NFD or HFD diet ($n = 5$ for all groups). (**b**) Euglycemic-hyperinsulinemic clamp procedure in 12-week-old wild-type mice treated with CTRLi vector ($n = 5$; white) or RANKi vector ($n = 5$; black) after 4 weeks of HFD. Gray bars indicate wild-type mice receiving NFD. Data (**a**,**b**) are shown as the means ± s.e.m. $^*P < 0.05$, $^{**}P < 0.01$ compared to controls calculated using the Mann Whitney *U* test. (**c**) Western blots showing Akt phosphorylation (insulin signaling) (pAkt) in hepatic tissue taken from 12-week-old control *Rank*^{WT} and *Rank*^{LKO} mice fed an HFD. (**d**) Western blots showing expression of phosphorylated RelA (p-RelA), total RelA, phosphorylated IKK-α and IKK-β (pIKKα/β), total IKK-α, total IKK-β and glyceraldehyde-3-phosphate dehydrogenase (GAPDH; loading control) in hepatic tissue of 12-week-old wild-type mice treated with CTRLi or RANKi vector and receiving HFD for 4 weeks.

There is strong evidence in previous literature that NF-κB activation is an initial and crucial step in the evolution of T2DM contributing to both hepatic insulin resistance and β-cell apoptosis, and providing a link between overnutrition, metabolic inflammation and impaired autophagy in the hypothalamus and the development of obesity[1,3,5,6,25,26]. Under resting conditions, NF-κB forms a complex with the inhibitory subunit IκB. Phosphorylation and proteasome-mediated degradation of IκB by IKKs releases NF-κB for translocation into the nucleus and promotes transcription of genes encoding inflammatory mediators. Activation of NF-κB is elicited by a broad spectrum of conditions featuring the diabetic milieu, including hyperglycemia, oxidative stress and high concentrations of fatty acids[1]. Transgenic LIKK mice characterized by a twofold upregulation of NF-κB as a result of selective overexpression of IKK-β in the liver develop a T2DM phenotype in the absence of the aforementioned conditions[5]. Conversely, genetic disruption of NF-κB signaling effectively protects diabetes-prone mice from the development of metabolic abnormalities[5], and pharmacological inhibition of IKK-β improves insulin resistance in mice and patients with T2DM[27]. Apart from canonical IKK–NF-κB pathways, the noncanonical NF-κB–inducing kinase–NF-κB pathway has been implicated in glucose intolerance of obese mice[28], and direct involvement of NF-κB in the control of energy sensing and homeostasis (mitochondrial respiration) has been proposed[29].

Here the concentration of soluble RANKL, a prototypic activator of NF-κB, emerged as a significant risk predictor of T2DM in the general community ($P < 0.001$). The association was independent of age, sex and other determinants of T2DM, was internally consistent

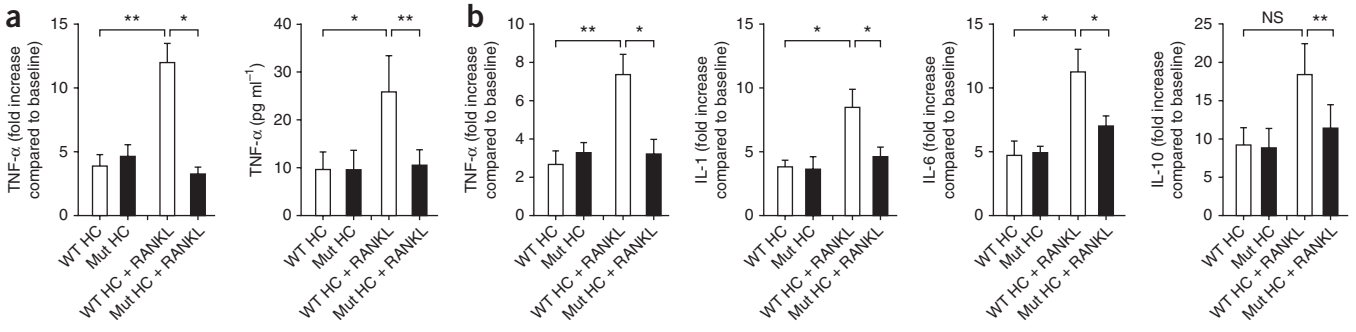

Figure 3 Effects of RANKL-stimulated hepatocytes on Kupffer cell activation. (**a**) TNF-α mRNA expression (real-time PCR analysis; left) and protein amounts (ELISA; right) in hepatocytes of 12-week-old control *Rank*^{WT} (WT HC) and *Rank*^{LKO} (Mut HC) mice either unstimulated or stimulated with RANKL (50 ng ml^{-1}) ($n = 5$ for all groups). (**b**) Real-time PCR analysis of TNF-α, IL-1, IL-6 and IL-10 mRNA expression in cultured Kupffer cells of wild-type mice after exposure to supernatants from unstimulated and RANKL-stimulated (50 ng ml^{-1}) WT HC or Mut HC mice ($n = 5$ for all groups). Data are shown as the means ± s.e.m. NS, not significant, $^*P < 0.05$, $^{**}P < 0.01$ compared to control calculated using the Mann Whitney *U* test.

within subgroups and showed a dose-response pattern. Whereas previous prospective studies on the association of soluble RANKL concentration and T2DM are lacking, a number of evaluations have yielded evidence of higher OPG concentrations among patients with prevalent T2DM[8–11]. Our study indicates that elevation of OPG concentration does not precede T2DM but rather emerges with or after disease occurrence, which is consistent with observations in mice after induction of diabetes with streptozotocin[30]. Our epidemiological findings are corroborated by a large number of mouse and *in vitro* studies. We use five different *in vivo* approaches to downregulate RANKL signaling in nutritional (HFD) and genetic (*ob/ob*) mouse models of insulin resistance and T2DM, which consistently revealed a marked improvement in hepatic insulin sensitivity and amelioration or even normalization of glucose concentrations and tolerance and insulin signaling. Notably, it is sufficient to block Rank, the cognate receptor of RANKL, in hepatocytes and liver tissue to elicit antidiabetic effects, as demonstrated by either hepatocyte-specific knockout of *Rank* ($Rank^{LKO}$) or liver-specific blockade of Rank expression by hydrodynamic injection of RANKi vectors, a technique that is highly effective in expressing or silencing proteins in the liver[20–23].

Our data establish the liver as a RANKL-responsive organ. Binding of RANKL to its cognate receptor RANK activates NK-κB signaling in hepatocytes, leading to cytokine production, Kupffer cell activation, excess storage of fat and manifestation of insulin resistance. The skeletal and immune systems are considered key sources of RANKL in humans and have both been linked to T2DM[31–35].

The crosstalk between bone and glucose metabolism involves osteocalcin and RANKL. The former is a product of mature osteoblasts and improves insulin resistance, while also protecting against the development of diabetes mellitus[31,32]. The latter is a product of immature osteoblast-lineage cells and osteocytes and impairs glucose tolerance (this study). In accordance with this concept, markers of bone resorption correlate with insulin resistance in gestational diabetes, and glucocorticoid therapy, with its well-known diabetogenic effects, blocks osteoblast maturation, osteocalcin expression and simultaneously enhances RANKL expression[33]. It can be hypothesized that the opposing functions of RANKL and osteocalcin in bone extend to glucose homeostasis.

The other major source of RANKL is the immune system involving activated T cells[34] and other cell lines capable of adopting a proinflammatory phenotype, for example, endothelial cells[35] or adipocytes, which express not only TNF-α but also RANKL[36] and enhance RANKL production as a result of stimulation with TNF-α. Of note, systemic inflammation and endothelial cell activation, as well as obesity and adipose tissue inflammation, are common features and precursors of T2DM. It is still unknown to what extent the skeleton and the immune systems may contribute to hepatic insulin resistance; however, both sources of RANKL are connected in that immune activation triggers bone resorption and inhibits bone formation, as well as osteocalcin expression[37].

Overall, our epidemiological and experimental data support the conclusion that RANKL signaling has a role in the pathogenesis of hepatic insulin resistance and T2DM and provides a link between inflammation and disrupted glucose homeostasis. These findings hold promise for the future development of new therapeutic and preventive approaches. Notably, thiazolidinediones and angiotensin-receptor blockers, which have been reported to lower the incidence of T2DM[38], are known to lower RANKL activity. Moreover, metformin, the most commonly used antidiabetic drug worldwide, effectively downregulates RANKL expression in bone tissue[39,40]. Interventions specifically targeting RANKL to prevent or treat T2DM are currently restricted to mice, but studies in humans are a next logical step to pursue. The currently available knowledge on RANKL antagonism in the treatment of osteoporosis may help to design pharmacological strategies suitable for improving hepatic insulin sensitivity in the liver.

METHODS

Methods and any associated references are available in the online version of the paper.

Note: Supplementary information is available in the online version of the paper.

ACKNOWLEDGMENTS

This study was supported by the Deutsche Forschungsgemeinschaft (SPP1468-IMMUNOBONE to G.S.), the Bundesministerium für Bildung und Forschung (Bundesministerium für Bildung und Forschung project ANCYLOSS to G.S.), the European Union (Masterswitch to G.S.), the Innovative Medicines Initiative funded project BTCure (to G.S.), the National Institute of Diabetes and Digestive and Kidney Diseases (K24 DK080140 to J.B.M.), the Genomics of Lipid-associated Disorders of the Austrian Genome Research Programme GEN-AU (to F.K.), the 'Pustertaler Verein zur Prävention von Herz- und Hirngefässerkrankungen', the 'Gesundheitsbetrieb Bruneck' and the 'Assessorat für Gesundheitswesen, Familie und Soziales, Bolzano'. G.M. is recipient of the Umberto Di Mario Prize by the Società Italiana di Diabetologia 2011. A.G. was supported by grants from Fondazione Don Gnocchi, Università Cattolica del Sacro Cuore (Fondi Ateneo Linea D.3.2 Sindrome Metabolica) and the Italian Ministry of Education, University and Research (PRIN 2010JS3PMZ_011). A.M. and H.T. were supported by the Christian Doppler Research Society. E.B. is recipient of grants from the Italian Ministry of Education, University and Research and the University of Verona. J.M.P. holds an advanced European Research Council grant and is supported by the Austrian Academy of Sciences, a Grant by the National Bank Foundation and Era of Hope/US Department of Defense. We thank B. Enrich for technical support.

AUTHOR CONTRIBUTIONS

S.K., G.S. and J. Willeit had the idea for this research, took responsibility for the epidemiological and experimental design of this work and wrote the manuscript. G.S. designed all analyses for the experiments. S.K. and P.W. performed all analyses of the epidemiological portion of the study and were supported by M.K. J. Willeit is the principle investigator of the Bruneck Study. J. Wittman, A.G., A.B., A.R.M., G.M., G.P.S., T.K., S.W., J.L., D.M., U.B. and H.T. performed the *in vitro* and *in vivo* experimental analysis. A.G., G.M. and G.P.S. performed the animal clamp studies and contributed to the interpretation of the data. G.E., A.M. and F.O. participated in data collection, laboratory analyses, fund raising and conception of the Bruneck Study. M.S. and F.K. performed genetic analyses and contributed to the interpretation of these data. E.B. contributed to researching data. E.B. and J.B.M. gave their advice regarding study design and analysis. J.M.P. and M.O. conducted the experiments involving *Msk-Rank* and *Rip-Rank* mice. E.B., J.B.M., H.T., A.G., J.M.P. and all other authors made a critical revision of the final manuscript.

COMPETING FINANCIAL INTERESTS

The authors declare competing financial interests: details are available in the online version of the paper.

Published online at http://www.nature.com/doifinder/10.1038/nm.3084.
Reprints and permissions information is available online at http://www.nature.com/reprints/index.html.

1. Mazzone, T., Chait, A. & Plutzky, J. Cardiovascular disease risk in type 2 diabetes mellitus: insights from mechanistic studies. *Lancet* **371**, 1800–1809 (2008).
2. Targher, G., Day, C.P. & Bonora, E. Risk of cardiovascular disease in patients with nonalcoholic fatty liver disease. *N. Engl. J. Med.* **363**, 1341–1350 (2010).
3. Shoelson, S.E., Herrero, L. & Naaz, A. Obesity, inflammation, and insulin resistance. *Gastroenterology* **132**, 2169–2180 (2007).
4. Donath, M.Y. *et al.* Mechanisms of β-cell death in type 2 diabetes. *Diabetes* **54** (suppl. 2), S108–S113 (2005).
5. Cai, D. *et al.* Local and systemic insulin resistance resulting from hepatic activation of IKK-β and NF-κB. *Nat. Med.* **11**, 183–190 (2005).
6. Arkan, M.C. *et al.* IKK-β links inflammation to obesity-induced insulin resistance. *Nat. Med.* **11**, 191–198 (2005).
7. Anderson, D.M. *et al.* A homologue of the TNF receptor and its ligand enhance T-cell growth and dendritic-cell function. *Nature* **390**, 175–179 (1997).
8. Venuraju, S.M., Yerramasu, A., Corder, R. & Lahiri, A. Osteoprotegerin as a predictor of coronary artery disease and cardiovascular mortality and morbidity. *J. Am. Coll. Cardiol.* **55**, 2049–2061 (2010).

9. Kiechl, S. *et al.* The osteoprotegerin/RANK/RANKL system: a bone key to vascular disease. *Expert Rev. Cardiovasc. Ther.* **4**, 801–811 (2006).
10. Lieb, W. *et al.* Biomarkers of the osteoprotegerin pathway. Clinical correlates, subclinical disease, incident cardiovascular disease, and mortality. *Arterioscler. Thromb. Vasc. Biol.* **30**, 1849–1854 (2010).
11. Kiechl, S. *et al.* Osteoprotegerin is a risk factor for progressive atherosclerosis and cardiovascular disease. *Circulation* **109**, 2175–2180 (2004).
12. Collin-Osdoby, P. Regulation of vascular calcification by osteoclast regulatory factors RANKL and osteoprotegerin. *Circ. Res.* **95**, 1046–1057 (2004).
13. Semb, A.G. *et al.* Osteoprotegerin and soluble receptor activator of nuclear factor-κB ligand and risk for coronary events: a nested case-control approach in the prospective EPIC-Norfolk population study 1993–2003. *Arterioscler. Thromb. Vasc. Biol.* **29**, 975–980 (2009).
14. Kiechl, S. *et al.* Soluble receptor activator of nuclear factor-κ B ligand and risk for cardiovascular disease. *Circulation* **116**, 385–391 (2007).
15. Schett, G. *et al.* Soluble RANKL and risk of nontraumatic fracture. *J. Am. Med. Assoc.* **291**, 1108–1113 (2004).
16. Terpos, E. *et al.* Soluble receptor activator of nuclear factor κB ligand-osteoprotegerin ratio predicts survival in multiple myeloma: proposal for a novel prognostic index. *Blood* **102**, 1064–1069 (2003).
17. Ziolkowska, M. *et al.* High levels of osteoprotegerin and soluble receptor activator of nuclear factor κ B ligand in serum of rheumatoid arthritis patients and their normalization after anti-tumor necrosis factor α treatment. *Arthritis Rheum.* **46**, 1744–1753 (2002).
18. Moschen, A.R. *et al.* The RANKL/OPG system is activated in inflammatory bowel disease and relates to the state of bone loss. *Gut.* **54**, 479–487 (2005).
19. Shimizu, H. *et al.* Angiotensin II accelerates osteoporosis by activating osteoclasts. *FASEB J.* **22**, 2465–2475 (2008).
20. Nishikawa, M., Nakayama, A., Takahashi, Y., Fukuhara, Y. & Takakura, Y. Reactivation of silenced transgene expression in mouse liver by rapid, large-volume injection of isotonic solution. *Hum. Gene Ther.* **19**, 1009–1020 (2008).
21. Liu, F., Song, Y. & Liu, D. Hydrodynamics-based transfection in animals by systemic administration of plasmid DNA. *Gene Ther.* **6**, 1258–1266 (1999).
22. Yang, P.L., Althage, A., Chung, J. & Chisari, F.V. Hydrodynamic injection of viral DNA: a mouse model of acute hepatitis B virus infection. *Proc. Natl. Acad. Sci. USA* **99**, 13825–13830 (2002).
23. Jiang, J., Yamato, E. & Miyazaki, J. Intravenous delivery of naked plasmid DNA for *in vivo* cytokine expression. *Biochem. Biophys. Res. Commun.* **289**, 1088–1092 (2001).
24. Huang, W. *et al.* Depletion of liver Kupffer cells prevents the development of diet-induced hepatic steatosis and insulin resistance. *Diabetes* **59**, 347–357 (2010).
25. Meng, Q. & Cai, D. Defective hypothalamic autophagy directs the central pathogenesis of obesity via the IκB kinase β (IKKβ)/NF-κB pathway. *J. Biol. Chem.* **286**, 32324–32332 (2011).
26. Cai, D. & Liu, T. Inflammatory cause of metabolic syndrome via brain stress and NF-κB. *Aging (Albany, NY)* **4**, 98–115 (2012).
27. Hundal, R.S. *et al.* Mechanism by which high-dose aspirin improves glucose metabolism in type 2 diabetes. *J. Clin. Invest.* **109**, 1321–1326 (2002).
28. Sheng, L. *et al.* NF-κB–inducing kinase (NIK) promotes hyperglycemia and glucose intolerance in obesity by augmenting glucagon action. *Nat. Med.* **18**, 943–949 (2012).
29. Mauro, C. *et al.* NF-κB controls energy homeostasis and metabolic adaptation by upregulating mitochondrial respiration. *Nat. Cell Biol.* **13**, 1272–1279 (2011).
30. Secchiero, P. *et al.* An increased osteoprotegerin serum release characterizes the early onset of diabetes mellitus and may contribute to endothelial cell dysfunction. *Am. J. Pathol.* **169**, 2236–2244 (2006).
31. Lee, N.K. *et al.* Endocrine regulation of energy metabolism by the skeleton. *Cell* **13**, 456–469 (2007).
32. Kanazawa, I. *et al.* Serum osteocalcin level is positively associated with insulin sensitivity and secretion in patients with type 2 diabetes. *Bone* **48**, 720–725 (2011).
33. Brennan-Speranza, T.C. *et al.* Osteoblasts mediate the adverse effects of glucocorticoids on fuel metabolism. *J. Clin. Invest.* **122**, 4172–4189 (2012).
34. Kong, Y.Y. *et al.* Activated T cells regulate bone loss and joint destruction in adjuvant arthritis through osteoprotegerin ligand. *Nature* **402**, 304–309 (1999).
35. Kindle, L. *et al.* Human microvascular endothelial cell activation by IL-1 and TNF-α stimulates the adhesion and transendothelial migration of circulating human $CD14^+$ monocytes that develop with RANKL into functional osteoclasts. *J. Bone Miner. Res.* **21**, 193–206 (2006).
36. Goto, H. *et al.* Primary human bone marrow adipocytes support TNF-α–induced osteoclast differentiation and function through RANKL expression. *Cytokine* **56**, 662–668 (2011).
37. Bertolini, D.R. *et al.* Stimulation of bone resorption and inhibition of bone formation *in vitro* by human tumour necrosis factors. *Nature* **319**, 516–518 (1986).
38. Nathan, D.M. Navigating the choices for diabetes prevention. *N. Engl. J. Med.* **362**, 1533–1535 (2010).
39. Liu, L., Zhang, C., Hu, Y. & Peng, B. Protective effect of metformin on periapical lesions in rats by decreasing the ratio of receptor activator of nuclear factor κ B ligand/osteoprotegerin. *J. Endod.* **38**, 943–947 (2012).
40. Mai, Q.G. *et al.* Metformin stimulates osteoprotegerin and reduces RANKL expression in osteoblasts and ovariectomized rats. *J. Cell Biochem.* **112**, 2902–2909 (2011).

ONLINE METHODS

Study population. The Bruneck Study is a prospective population-based survey on the epidemiology and pathogenesis of atherosclerosis and related traits[11,14,15,41,42]. The study protocol was approved by the ethics committees of Bolzano and Verona, and all study subjects gave their written informed consent. At the study baseline in 1990, we recruited the study population as a random sample of all inhabitants of Bruneck stratified according to sex and age (between age 40 and 79 years, with 125 women and 125 men in each decade of age; n = 1,000 total). The participation rate was 93.6%, with data assessment completed in 919 subjects and measurements of soluble RANKL concentrations available in 909 subjects[11,14,15]. We excluded 65 subjects with a baseline diagnosis of T2DM, leaving a study population of 844 for the current analysis. Follow-up examinations were performed every 5 years, with participation rates exceeding 90%. Of all subjects, including those who did not participate in or died during follow up, full medical records were available for review (100% follow up for clinical endpoints).

Clinical history and examination. We assessed risk factors by validated standard procedures described previously[11,14,15,41,42]. Body mass index was calculated as weight divided by height squared. Waist and hip circumferences were measured by a plastic tape meter at the level of the umbilicus and the greater trochanters. The activity score was composed of the scores for work (three categories) and sports or leisure activities (0, ≤2 or >2 h per week). We defined socioeconomic status on a three-category scale (low, medium or high) on the basis of information about occupational status and educational level of the person with the highest income in the household. High socioeconomic status was assumed if the participant had ≥12 years of education or an occupation with an average monthly income ≥$2,000 (1990 salary). Low socioeconomic status was defined by ≤8 years of education or an average monthly income ≤$1,000. Family history of T2DM refers to first-degree relatives.

We established the diagnosis of T2DM according to American Diabetes Association criteria (fasting glucose ≥126 mg dl^{-1} (7 mmol l^{-1}) or when the subjects had a clinical diagnosis of T2DM and received antidiabetic treatment (diet or drugs)). Self-reported T2DM status was confirmed by reviewing the medical records of the subject's general practitioners and Bruneck Hospital. A major strength of the Bruneck Study is that virtually all participants living in the survey area were referred to the same hospital and the network existing between hospital and practitioners allowed the retrieval of full medical information. In ancillary analyses, we applied HbA1c-based diagnostic criteria of T2DM (HbA1c ≥6.5%)[43]. There were no cases of type 1 diabetes in this cohort.

We estimated the degree of insulin sensitivity by homeostasis model assessment (HOMA)[44]. In particular, we computed an insulin resistance score (HOMA-IR) with the formula fasting plasma glucose (mmol l^{-1}) × fasting serum insulin (mU l^{-1}) × 22.5^{-1}. High HOMA-IR values indicate insulin resistance. Gutt insulin sensitivity index at 0 and 120 min ($ISI_{0,120}$) was calculated as detailed previously[45]. This index measures insulin sensitivity, so for the present analysis, we used the inverse (ISI^{-1}). We estimated the β-cell secretory response to oral glucose load using baseline GTT data as described by Sluiter and coworkers[46] and assessed metabolic syndrome and its components according to National Cholesterol Education Program Adult Treatment Panel III criteria.

Serum OPG and soluble RANKL. Blood samples were drawn after an overnight fast and 12 h of abstinence from smoking and immediately processed or frozen and stored at −70 °C. All samples were handled in exactly the same way and assayed in a random sequence. The technician who performed the measurement of soluble RANKL concentration was not aware of the subject characteristics, including diabetes status. Samples taken in 1990 and 1995 were analyzed in 2000 after 10 and 5 years of storage, respectively (without any thawing-freezing cycle), and samples taken in 2000 were immediately processed[11,14,15]. High consistency in the absolute concentrations of RANKL and OPG in the three assessments indicated long-term stability of these molecules under the storage conditions applied[11,14,15]. We measured OPG concentration using a sandwich enzyme immunoassay[11]. This assay detects both monomeric and dimeric forms of OPG, including OPG bound to its ligand, and has a lower detection limit of 0.14 pmol l^{-1} and intra- and inter-assay variability of <10%. We measured serum concentrations of soluble uncomplexed RANKL with a commercial sandwich-type assay (Biomedica)[14,15]. In this assay, chimeric OPG-Fc protein was coated on microtiter plates and used to bind free RANKL in the samples. In a second step, RANKL captured by OPG was detected with a specific affinity-purified and biotinylated rabbit antibody followed by incubation with streptavidin peroxidase and visualization with tetramethylbenzidine. Biosynthetic soluble RANKL diluted in human serum was used as standard material. We used signal amplification to achieve a lower detection limit of 0.08 pmol l^{-1}, allowing for the measurement of RANKL in virtually all subjects. The intra- and inter-assay coefficients of variation were 5% and 8%, respectively.

Statistical analyses of epidemiological data. Statistical calculations were performed using SPSS 18.0 (SPSS) and Stata 12 (Stata) and adhered to predefined protocols. Person years of follow up for each participant were accrued from the baseline in 1990 until diagnosis of T2DM, death or October 1, 2005, whichever came first. We divided the participants into three approximately equally sized groups according to tertiles of RANKL concentration and used the bottom tertile group as the reference category. Separate models treated RANKL concentration as a continuous variable. Given its skewed distribution, $\log_e$-transformed concentrations of soluble RANKL were used throughout the manuscript to minimize the effect of extreme observations. When additionally excluding outliers (RANKL concentrations >3 s.d. above or below the mean or >95th (<5th) percentile), the results were very similar. We assessed the association between RANKL concentration and incident T2DM by pooled logistic regression analysis[47]. This technique treated each observation period (1990–1995, 1995–2000 and 2000–2005) as a mini follow-up study in which updated risk factor measurements were used to predict T2DM risk. Observations over the various periods were pooled into a single sample. Subjects who developed T2DM were censored with respect to subsequent follow up. This approach has been shown to be asymptotically equivalent to a Cox regression analysis with time-dependent covariates in the case of short intervals between re-evaluations and low rates of events[47]. We performed sensitivity analyses for a 20-year follow up using 2000 RANKL concentrations to predict T2DM risk between 2005 and 2010. Base models were adjusted for age, sex and follow-up period. Multivariate models were additionally adjusted for social status, cigarette smoking, alcohol consumption, physical activity and family history of diabetes (model 1), plus body mass index and waist-to-hip ratio (model 2), plus fasting glucose (or HbA1c) and $\log_e$-transformed hsCRP (model 3), plus common types of medication (model 4). All reported P values were two sided.

Cloning of RANKi expression vectors. We designed shRNAs against mouse *Rank* (GenBank accession NM_009399) and cloned them according to the procedures of the RNAi consortium (http://www.broadinstitute.org/rnai/trc). In brief, the lentiviral vector pLKO.1 (ref. 48) was digested with the restriction enzymes AgeI and EcoRI (New England Biolabs) and gel purified (gel extraction kit, QIAGEN). Single-stranded oligonucleotides encompassing future RANKi were ordered (Invitrogen) and annealed to form double-stranded DNA molecules with AgeI- and EcoRI-compatible overhangs. Correct clones were identified by restriction digests and confirmed by sequencing analysis (Seqlab).

Cloning of a mouse RANKi 3×Flag-tagged expression vector. We isolated total RNA from splenic mouse cells (RNeasy kit, QIAGEN) and used 2 µg for the generation of complementary DNA (cDNA) (RevertAid Premium First Strand cDNA Synthesis Kit, Fermentas). The 1.9-kb mouse *Rank* (m*Rank*) transcript was amplified with the primers m*Rank* real-time PCR forward (5′-GAGCTAGCACCATGGCCCCGCGCGCCCGG-3′) and m*Rank* real-time PCR reverse (5′-GAAAGCTTTTCTGCACATTGTCCGGACCC-3′; all primers from Invitrogen), digested with restriction enzymes NheI and HindIII (NEB) and cloned into a modified eukaryotic expression vector pcDNA3 (Invitrogen) containing a triple Flag tag downstream of the multiple cloning site to yield C-terminal Flag-tagged mouse Rank proteins. We identified correct clones by sequencing the complete m*Rank* insert (Seqlab).

Testing of RANKi knockdown efficiency. We seeded 10^5 HEK293 cells in 24-well plates in 1 ml DMEM supplemented with 10% FCS (both from

doi:10.1038/nm.3084

Invitrogen) and maintained them at 37 °C and 7.5% CO_2 in a humidified incubator. After 24 h, we transfected cells with FuGeneHD transfection reagent (Roche Applied Science) according to the manufacturer's instructions. For each well, 50 ng RANKi 3×Flag expression vector, 400 ng of the different RANKi vectors and 50 ng of a modified peGFP-C1 plasmid (Clontech) encoding an enhanced GFP (eGFP) fusion protein of 65 kDa to demonstrate that equal transfection efficiencies were used. Twenty-four hours after transfection, cells were washed twice in PBS and lysed in Laemmli sample buffer. Proteins were separated by 12.5% SDS-PAGE, blotted onto a nitrocellulose membrane (Whatman Schleicher and Schuell) by semi-dry blotting, and the membrane was stained with Ponceau S to check for transfer efficiency and assess loading of equal protein amounts. After blocking the membrane in 5% milk in Tris-buffered saline with 0.1% Tween-20 (TBST), the membranes were stained stepwise with mouse antibody to Flag (1:1,000 dilution in TBST, catalog number F3165, Sigma) and mouse antibody to GFP (1:1,000 dilution in TBST, catalog number 11814460001, Roche Applied Science) and developed with a horseradish peroxidase (HRP)-conjugated goat anti-mouse secondary antibody (1:20,000 dilution in TBST with 5% milk, catalog number 172-1011, Bio-Rad) and the enhanced chemiluminescence method.

Mouse diabetes models. The animal studies were approved by the Animal Ethics Committee of the University of Erlangen-Nuremberg. We obtained female 8-week-old leptin-deficient (*ob/ob*) mice[49] from Jackson Laboratories. To block RANKL signaling, we treated the mice with recombinant mouse Opg (Amgen) at a dose of 10 mg per kg body weight three times per week or vehicle (PBS) for 6 weeks ($n = 8$ per group). Alternatively, mice were treated with the aforementioned RANKi vector (20 μg) or the respective CTRLi vector (20 μg) by hydrodynamic injection of a volume of 2 ml into the tail vein (rate, 0.4 ml s^{-1}) at days 1 and 14. Mice were analyzed 28 d after the first injection. The technique of hydrodynamic injection, which allows vector-based regulation of gene expression, has been described previously[20–23]. Hydrodynamic injection was also applied to an alternative well-established animal model of insulin resistance and diabetes[50], which is based on HFD. The same shRNA vectors and protocols were used. HFD D12331 was derived from Research Diets (New Brunswick). In addition, two genetic models to selectively block Rank in hepatocytes were established. Conditional *Rank* knockout mice ($Rank^{KO}$) were interbred with another transgenic mouse expressing the Cre recombinase under the hepatocyte-specific albumin promoter. We subjected the resulting $Rank^{LKO}$ mice to NFD or HFD or crossed them with *ob/ob* mice to obtain $Rank^{LKO}$ *ob/ob* mice.

Euglycemic-hyperinsulinemic clamp technique. We performed clamp procedures in (i) $Rank^{LKO}$ and $Rank^{WT}$ mice fed an NFD or HFD and (ii) wild-type mice fed an NFD or HFD and receiving treatment with either CTRLi vector or RANKi vector. For the clamp procedure, we anesthetized mice 3–5 d before the test using an intraperitoneal (i.p.) injection of xylazine and ketamine, inserted an indwelling catheter into the right internal jugular vein and extended it to the level of the right atrium. The catheter was filled with heparin and saline, sealed and tunneled subcutaneously around the side of the neck to the back of the head. The catheter was externalized through a skin incision. Immediately after surgery, mice were housed in individual cages and subjected to a standard light (6 a.m. to 6 p.m.) and dark (6 p.m. to 6 a.m.) cycle[51–53]. Mice were studied after a 6-h fast in an awake and unrestrained state using the euglycemic-hyperinsulinemic clamp technique. To determine basal and insulin-stimulated rates of endogenous glucose production (rate of glucose appearance, R_a), a prime continuous infusion of HPLC-purified [3–3H]glucose (10 μCi bolus; 0.1 μCi min^{-1}) was started at –60 min and maintained throughout the 90-min insulin clamp study. At time 0, a primed continuous (4.0 mU per kg body weight per min) infusion of human insulin was started simultaneously with a variable infusion of 20% dextrose to maintain the plasma glucose concentration constant at its basal level. Plasma samples for determination of [3–3H]glucose–specific activity were obtained at times –20, –10 and 0 min during the basal period and at 60, 70, 80 and 90 min during the insulin-clamp period. Data for total-body glucose uptake and endogenous glucose production (R_a) represent the mean values during the last 20 min of the basal period and during the last 30 min of the insulin-clamp period when the steady-state plateau of [3–3H]glucose radioactivity was achieved. Under steady-state conditions, the rate of total-body glucose disappearance (R_d) equals the rate of glucose appearance (R_a) and is calculated by dividing the infusion rate of [3–3H]glucose (dpm per kg body weight per min) by the steady-state plateau of [3–3H]glucose–specific activity (dpm mg^{-1}). The rate of endogenous glucose production is calculated by subtracting the exogenous glucose infusion rate from the rate of total-body glucose appearance (R_a)[54]. Our clamp procedure was designed to reveal hepatic differences. For a focus on skeletal muscle differences, a clamp procedure with higher insulin infusion rates and complete suppression of endogenous glucose production would be the method of choice.

GTT and ITT. Mice fed an NFD or HFD were fasted for 16–18 h before receiving 1 mg glucose per g body weight by i.p. injection. Blood was collected from the tail vein at 0, 30, 60 and 120 min after the glucose load. For testing insulin tolerance, mice were fasted for 4 h before applying 5.5 IU human insulin per kg body weight i.p. (Eli Lilly). We calculated the rate constant for plasma glucose disappearance (K_{ITT}) with the formula $0.693 \times t_{1/2}^{-1}$. The plasma glucose $t_{1/2}$ was calculated from the slope of least-square analysis of the plasma glucose concentrations during the first 15 min after insulin injection, when the plasma glucose concentration declines linearly[55].

Western blot analysis. We collected liver, muscle and adipose tissue from (i) wild-type mice receiving HFD and treatment with either CTRLi vector or RANKi vector and (ii) $Rank^{LKO}$ and $Rank^{WT}$ mice fed an HFD. Tissue was homogenized by 20 mM Tris-HCl, pH 7.4, 1% SDS and 1:10 of a protease inhibitor cocktail (Sigma), and protein extracts were boiled and separated by SDS-PAGE and then transferred onto nitrocellulose membrane after the removal of cell debris by centrifugation. After blocking with Tris-buffered saline, 0.1% Tween 20 and 5% nonfat dry milk, membranes were incubated with primary antibodies to RANKL (clone L300, 1:1,000, Cell Signaling), Rank (clone #4845, 1:1,000, Cell Signaling), Opg (clone BTF3L1, 1:1,000, Novus Biologicals), pRelA (clone 93H1, 1:1,000), total RelA (clone C22B4, 1:1,000), pIKK-α/IKK-β (clone 16A6, 1:1,000) total IKK-α (#2682, 1:1,000), total IKK-β (clone L570, 1:1,000) and GAPDH (clone 14C10, 1:1,000) (all Cell Signaling, Beverly, MA). For detection of insulin signaling, we analyzed liver tissues from $Rank^{LKO}$ and $Rank^{WT}$ mice fed an NFD or HFD for Akt phosphorylation. Mice were anesthetized, the portal vein was prepared and 10 IU human insulin per kg body weight (0.1 ml volume) was injected. After 5 min, the liver was removed, snap frozen and digested according to the protocol provided. Protein extracts were subjected to western blotting, and the expression of pAkt (clone L32A4, 1:1,000) and total Akt (clone 40D4, 1:1,000) were detected by the respective antibodies (Cell Signaling).

Hepatic triglycerides and cholesterol. We extracted lipids from liver tissues of $Rank^{LKO}$ and $Rank^{WT}$ mice as described previously[56]. Dried lipid extracts were dissolved in 1% Triton X-100 in chloroform, exposed to liquid nitrogen and dissolved in H_2O as described[57]. Enzymatic kits (Wako Chemicals) were used for the determination of triglycerides and total cholesterol content.

RT-PCR of liver tissue. We extracted total RNA from liver tissue and hepatocytes using TRIzol reagent (Invitrogen) followed by DNase-I digestion. A total of 1 μg of purified RNA was used for the synthesis of cDNA with a Reverse Transcription System Kit (Applied Biosystems). Quantitative real-time PCR for RANKL, Rank and Opg was performed using LightCycler technology (Roche Diagnostics) and the Fast Start SYBR Green I kit for amplification and detection. The final amount of cDNA per reaction corresponded to 2.5 ng of total RNA used for reverse transcription. The expression of the target molecule was normalized to the expression of β-actin. Specific mRNA transcripts of TNF-α, IL-1β and CXCL1 were quantified with SYBR-Green and the ABI Prism 7000 Sequence Detection System (Applied Biosystems).

Hepatocyte isolation and stimulation. We isolated hepatocytes from naive C57BL/6, $Rank^{WT}$ and $Rank^{LKO}$ mice. After anesthesia and abdominal exploration, liver perfusion was performed through the vena cava with 50 ml perfusion buffer (8.3 g NaCl, 0.5 g KCl, 2.4 g 4-(2-hydroxyethyl)-1-piperazineethanesulfonic acid (HEPES), 5.5 ml 1 M NaOH and 2 ml 0.5 M

EGTA, pH 7.4). Then the liver was digested with 30 ml collagenase buffer (3.9 g NaCl, 0.5 g KCl, 0.7 g $CaCl_2 \times H_2O$, 24 g HEPES and 50 ml 1 M NaOH, pH 7.4) containing 1 mg liberase enzyme three (Roche Diagnostics, Basel, Switzerland). The digested liver was mashed *ex vivo*, and the resulting suspension was filtered through a 70-μm mesh and centrifuged on a Percoll density gradient centrifugation (VWR International) at 1,400*g* for 10 min. Hepatocytes were then plated on plastic plates (5×10^{-4} cells cm^{-1} cm^{-1}) and stimulated with 50 ng ml^{-1} mouse RANKL (R&D Systems) with or without the IKK-β–specific inhibitor AS602868 (10 μg ml^{-1}; kindly provided by Merck Serono). AS602868 is an anilinopyrimidine derivative and ATP competitor that selectively inhibits IKK-β.

Kupffer cell isolation. We perfused the livers of wild-type mice with calcium-free solution for 5 min and then perfused them with collagenase (Sigma-Aldrich). After centrifugation at 50*g*, the cell suspension was filtered through a 70-μm cell strainer (BD Biosciences). Then the solution was overlaid on Histopaque 1083 (Sigma-Aldrich) and centrifuged at 1,000*g* to remove hepatocytes. Phycoerythrin (PE)-conjugated antibody to F4/80 (clone BM8, 1:100, Biolegend) and anti-PE magnetic microbeads (Miltenyi) were then used for Kupffer cell isolation from the nonparenchymal cell fraction. Residual monocytes and neutrophils were depleted using antibodies to Gr-1 (clone RB6-8C5, 1:100, BD Biosciences).

41. Kiechl, S. *et al.* Toll-like receptor 4 polymorphisms and atherogenesis. *N. Engl. J. Med.* **347**, 185–192 (2002).
42. Bonora, E. *et al.* Population-based incidence rates and risk factors for type 2 diabetes in white individuals: the Bruneck study. *Diabetes* **53**, 1782–1789 (2004).
43. Gillett, M.J. International Expert Committee report on the role of the A1c assay in the diagnosis of diabetes: Diabetes Care 2009; 32(7): 1327–1334. *Clin. Biochem. Rev.* **30**, 197–200 (2009).
44. Bonora, E. *et al.* Homeostasis model assessment closely mirrors the glucose clamp technique in the assessment of insulin sensitivity: studies in subjects with various degrees of glucose tolerance and insulin sensitivity. *Diabetes Care* **23**, 57–63 (2000).
45. Gutt, M. *et al.* Validation of the insulin sensitivity index (ISI(0,120)): comparison with other measures. *Diabetes Res. Clin. Pract.* **47**, 177–184 (2000).
46. Sluiter, W.J., Erkelens, D.W., Reitsma, W.D. & Doorenbos, H. Glucose tolerance and insulin release, a mathematical approach I. Assay of the β-cell response after oral glucose loading. *Diabetes* **25**, 241–244 (1976).
47. D'Agostino, R.B. *et al.* Relation of pooled logistic regression to time dependent Cox regression analysis: the Framingham Heart Study. *Stat. Med.* **9**, 1501–1515 (1990).
48. Stewart, S.A. *et al.* Lentivirus-delivered stable gene silencing by RNAi in primary cells. *RNA* **9**, 493–501 (2003).
49. Furuhashi, M. *et al.* Treatment of diabetes and atherosclerosis by inhibiting fatty-acid–binding protein aP2. *Nature* **447**, 959–965 (2007).
50. Jornayvaz, F.R. *et al.* A high-fat, ketogenic diet causes hepatic insulin resistance in mice, despite increasing energy expenditure and preventing weight gain. *Am. J. Physiol. Endocrinol. Metab.* **299**, E808–E815 (2010).
51. Wang, L. *et al.* Peripheral disruption of the Grb10 gene enhances insulin signaling and sensitivity *in vivo*. *Mol. Cell Biol.* **27**, 6497–6505 (2007).
52. Giaccari, A. & Rossetti, L. Predominant role of gluconeogenesis in the hepatic glycogen repletion of diabetic rats. *J. Clin. Invest.* **89**, 36–45 (1992).
53. Giaccari, A. *et al. In vivo* effects of glucosamine on insulin secretion and insulin sensitivity in the rat: possible relevance to the maladaptive responses to chronic hyperglycaemia. *Diabetologia* **38**, 518–524 (1995).
54. Muse, E.D. *et al.* Role of resistin in diet-induced hepatic insulin resistance. *J. Clin. Invest.* **114**, 232–239 (2004).
55. Bonora, E. *et al.* Estimates of *in vivo* insulin action in man: comparison of insulin tolerance tests with euglycemic and hyperglycemic glucose clamp studies. *J. Clin. Endocrinol. Metab.* **68**, 374–378 (1989).
56. Bligh, E.G. & Dyer, W.J. A rapid method of total lipid extraction and purification. *Can. J. Biochem. Physiol.* **37**, 911–917 (1959).
57. Carr, T.P., Andresen, C.J. & Rudel, L.L. Enzymatic determination of triglyceride, free cholesterol, and total cholesterol in tissue lipid extracts. *Clin. Biochem.* **26**, 39–42 (1993).

doi:10.1038/nm.3084